Studies on the Topography of Biomembranes: Regioselective Photolabelling in Vesicles with the Tandem Use of Cholesterol and a Photoactivable Transmembrane Phospholipidic Probe

Yoichi Nakatani,* Masakuni Yamamoto, Yvonne Diyizou, William Warnock, Valérie Dollé, Wolfgang Hahn, Alain Milon, and Guy Ourisson

Abstract: ^{2}H NMR, DSC and UV studies of DMPC (1,2-dimyristoyl-*sn*-glycero-3-phosphocholine) vesicles have demonstrated the favourable physicochemical properties of the transmembrane phospholipid probes **1a** and **1b** for membrane topographical studies. In particular, in the presence of a physiological amount of cholesterol, only one transmembrane conformation is observed. The use of **1a** and cholesterol together for photolabelling experiments in DMPC vesicles led to a remarkable improvement in the regioselectivity of cross-linking between **1a** and DMPC, and between **1a** and cholesterol: the myristoyl chains functionalized at C11, C12 and C13 made up 95% of the total photolabelled myristates, and cholesterol was principally functionalized at the C25 position on the side-chain. This indicates the formation of a highly ordered bilayer structure and proves directly the orientation of cholesterol perpendicular to the membrane plane with its chain terminal buried in the middle of the bilayer.

Keywords
bilayers · cholesterol · membrane probes · phospholipids · photolabelling

Introduction

Cholesterol acts as a reinforcer of eucaryotic membranes.[1] It is assumed to be oriented perpendicularly to the plane of the bilayers, with its hydroxyl group in the water phase.[2] However, there have been few chemical studies bearing on the topography of cholesterol in membranes.[3] Even more importantly, the topography of membrane-bound proteins is known at atomic resolution only in exceptional cases.[4] Since the pioneering work of Khorana and Breslow[5] several groups have attempted to explore the internal structure of membranes by using photoreactive phospholipids or amphiphilic molecules, in the hope that photoirradiation of membranes containing them would lead to the formation of a covalent bond between the photophore and groups situated in proximity, thus labelling a definite level inside the bilayer. Although several *photoaffinity*-labelling studies have succeeded in determining the active sites of receptors that recognize their ligands,[6] there has been no success so far in the site-specific cross-linking of lipid chains or of proteins *within* phospholipid bilayers.[5] Both the yield of labelling and the site selectivity observed are very low in lipid–lipid interactions or in lipid-protein interactions.

By far the majority of photoreactive groups so far employed have been phenylazides, which produce nitrenes, and phenyldiazirines or diazo compounds, which produce carbenes. Although some new and promising photolabelling reagents have recently been developed in these classes,[7] the chemistry of nitrenes and carbenes is complex and presents several drawbacks in their use for *hydrophobic* photolabelling inside membranes: weak reactivity for C–H insertion (nitrenes), ready reaction with water (nitrenes, carbenes), other secondary reactions such as rearrangement (nitrenes, carbenes) and the thermal and light instability of their precursors. As we shall see below, these drawbacks can be circumvented by the use of benzophenones[6b].

Furthermore, the lack of regioselectivity in the photolabelling experiments described so far is certainly caused by the extensive disorder of the phospholipid matrix and/or the lipid probe itself above the phase transition temperature. Therefore, one of the keys for success in achieving highly depth-selective functionalization should be construction of a well-ordered bilayer system and a well-ordered probe.

Taking these points into consideration, we conceived and tested the tandem use of cholesterol (for its ordering effect on lipid chains) and the transbilayer photoactivable probe **1a** (and its deuterated derivative **1b**; Fig. 1) for the analysis of membrane topography.[8] The concept of the transmembrane structure was in fact suggested to us by the occurrence of membrane-spanning archaeal lipids (see for example structure **3** in Fig. 2).[9] The probe **1a** has the following desirable characteristics: 1) it is a phospholipid with polar groups at both terminals and a transmembrane chain whose length is about the same as the

[*] Prof. Y. Nakatani, Dr. M. Yamamoto, Dr. Y. Diyizou, Dr. W. Warnock, V. Dollé, W. Hahn, Prof. G. Ourisson
Laboratoire de Chimie Organique des Substances Naturelles associé au CNRS
Centre de Neurochimie, Université Louis Pasteur
5 rue Blaise Pascal, 67084 Strasbourg (France)
Telefax: Int. code + (88)607-620
e-mail: nakatani@chimie.u-strasbg.fr
Prof. A. Milon
Laboratoire de Pharmacologie et de Toxicologie Fondamentales, CNRS
Université Paul Sabatier, 118 route de Narbonne
31063 Toulouse (France)

  0947-6539/96/0202-0129 $ 10.00+.25/0

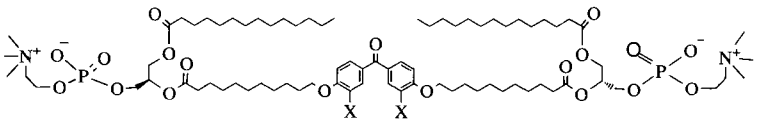

1a, X = H; **1b**, X = D

Fig. 1. Structure of photosensitive phospholipidic transmembrane probes **1a** and **1b**.

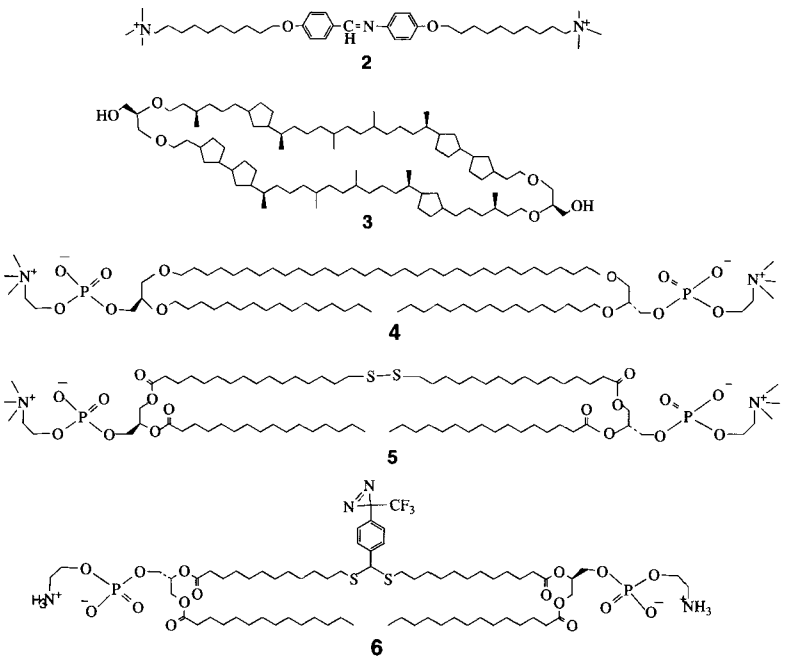

Fig. 2. Examples of dipolar amphiphilic molecules.

thickness of the lipid bilayer; 2) the photoreactive group is located on the transmembrane chain, so as to restrict its motion to a constant depth of the bilayer.

A 4,4′-alkoxybenzophenone was chosen as the photophore for the following reasons: 1) the efficiency of benzophenones in photochemical reactions has been well established theoretically and experimentally;[10] 2) benzophenones react preferentially with C–H bonds not only in organic solvents, but also in aqueous solutions including vesicles or micelles, that is, water can be considered as an inert solvent;[11] 3) benzophenones have a high quantum yield and 4,4′-dimethoxybenzophenone has approximately the same reactivity as benzophenone in the hydrogen abstraction of 2-propanol;[12] 4) benzophenones can be activated at 360 nm, which should avoid damage to proteins; 5) they are stable under normal laboratory lighting conditions and they are also chemically stable.

These desirable characteristics of benzophenones as photophores have been "rediscovered" and used especially to determine receptor–ligand binding sites.[13] Recently, phospholipidic probes carrying a benzophenone group at different positions on a fatty acyl chain have been employed for the analysis of the topography of bilayers.[14] A transmembrane probe bearing 3-trifluoromethyl-3-phenyl diazirine as a photophore has also been independently developed for the study of the topography of proteins in phospholipid bilayers[15] (see structure **6** in Fig. 2).

We present here some physicochemical properties of the probes **1a** and **1b** in lipid bilayers observed by UV, DSC (differential scanning calorimetry) and ^{2}H NMR methods. The results obtained permitted us to use the probe **1a** further for photochemical studies in several vesicle systems that will also be described here. Finally, the tandem use of the probe **1a** and cholesterol enabled us to achieve excellent regioselectivity of functionalization near the ends of lipid chains,[8b] and of cholesterol at the expected specific site (C25) on the side-chain. These studies are preliminary to work with membrane-bound proteins, which will be described later.

Abstract in French: *L'étude RMN ^{2}H, DSC et UV dans des bicouches de DMPC a montré que les sondes transmembranaires phospholipidiques* ***1a*** *et* ***1b*** *possèdent des propriétés physicochimiques favorables pour des études topographiques de membranes. En particulier, en présence d'une quantité "physiologique" de cholestérol, seule une conformation transmembranaire a été observée. L'utilisation concertée de la sonde* ***1a*** *et du cholestérol pour le photomarquage des vésicules de DMPC améliore remarquablement la régiosélectivité du couplage entre* ***1a*** *et le DMPC, et entre* ***1a*** *et le cholestérol: les chaînes myristoyles fonctionnalisées sur les positions C11, 12 et 13 représentent 95% du total des myristates marqués, et le cholestérol est principalement fonctionnalisé sur la position C25 de la chaîne. Ceci montre qu'il y a formation de bicouches très ordonnées et prouve directement que le cholestérol s'oriente perpendiculairement au plan de la membrane, la chaîne latérale étant positionnée au centre de la bicouche.*

Results and Discussion

1. Physicochemical studies of the transmembrane phospholipidic probes 1a and 1b in mixed vesicles with DMPC (1,2-dimyristoyl-*sn*-glycero-3-phosphocholine): The membrane properties of the probes **1a** and **1b** have been studied to answer the following questions: 1) Do they form vesicles with normal phospholipids? 2) Are the probes incorporated quantitatively into the membrane? 3) Are the probes well miscible with the phospholipid? 4) How are the probes located and oriented in the bilayer? 5) Does the presence of the probes influence the mobility of surrounding phospholipid chains?

Incorporation ratio of the probe in DMPC vesicles: We reconstituted vesicles with probe **1a** in admixture with DMPC and checked their formation by observation with an optical microscope (see Experimental Procedure). Attempts to prepare vesicles from the dipolar lipid **1a** alone resulted in the formation of a turbid liquid and microprecipitates, though DSC studies suggested the presence of multilamellar structures. The extent (average value per vesicle) of incorporation ("solubility") of probe **1a** in mixed vesicles with DMPC was measured by the methods described in the Experimental Procedure and expressed as s (mole% ratio), and r (equivalence% ratio to take into account the fact that probe **1a** corresponds to two normal phospholipid molecules); r represents approximately the volume% ratio occupied by the molecule **1a** in the mixed vesicles with DMPC (Table 1). At lower concentrations of compound **1a** ($s \leq 20$), almost complete incorporation into the vesicles occurred. How-

0947-6539/96/0202-0130 $ 10.00+.25/0 Chem. Eur. J. 1996, 2, No. 2

Table 1. Incorporation ratio of the probe **1a** in DMPC vesicles prepared by sonication.

Initial C_{1a} (mol%)	Incorporation ratio s [a]	r [a]
2	2	4
5	4	8
10	9	17
20	20	33
50	38 [b]	55 [b]

[a] s (mole% ratio) $=100\times C_{1a}/(C_{DMPC}+C_{1a})$ and r (equivalence% ratio) $=100\times 2C_{1a}/(C_{DMPC}+2C_{1a})$, where C_{1a} and C_{DMPC} are the molar concentrations of the probe **1a** and DMPC, respectively. [b] The value obtained from the first eluted fraction through Sepharose gel filtration of the crude vesicle preparation.

ever, when the molar% ratio of **1a** was increased to $s = 50$, total incorporation was not achieved.

Kunitake and Okahata[16] reported that the lamellar structure formed by the single-chain dipolar ammonium amphiphile **2** can be transformed into a vesicular structure by adding a second component, either didodecyldimethylammonium bromide or cholesterol. It has also been found that vesicles formed on addition of phosphatidylcholines or cholesterol to an archaebacterial di-bisphytanyltetraether **3** or a synthetic archaebacterial model compound **4**.[17, 18] In the present case, DMPC might play the same role in the DMPC/**1a** system as that of the second components above, that is, a "space-filling" role permitting the curvature required for vesicle formation.

Phases of multilamellar dispersions of DMPC and probe 1a: Differential scanning calorimetry (DSC) data were obtained from calorimetric heating scans of the hydrated pure components (**1a** and DMPC) and of mixtures of different molar fraction ratios (thermograms not shown here). A sharp thermal transition at 51 °C ($\Delta H = 70\ kJ\,mol^{-1}$) was observed for multilamellar dispersions of pure **1a**, and this can be identified as the main lipid bilayer transition (gel/liquid crystal phase transition). Another sharp transition was found for DMPC at 24 °C ($\Delta H = 20\ kJ\,mol^{-1}$), as already known ($T_m = 23.9$ °C, $\Delta H = 22\ kJ\,mol^{-1}$[19]), that is, the phase transition temperature (T_m) is higher for the transmembrane phosphocholine probe. Similar increased values of T_m were observed for other synthetic bis-phosphocholines (**4**, $T_m = 61.5$ °C, $\Delta H = 69\ kJ\,mol^{-1}$;[18] **5**, $T_m = 49$ °C, $\Delta H = 54\ kJ\,mol^{-1}$,[20] to be compared with $T_m = 41.4$ °C, $\Delta H = 36\ kJ\,mol^{-1}$ for DPPC (1,2-dipalmitoyl-*sn*-glycero-3-phosphocholine), Fig. 2).[19] The thermograms of mixtures of DMPC and **1a** reveal two phase transitions: a sharp one occurring in the same temperature range as that of pure DMPC, and a broad transition between the T_m's of the two lipids; no thermal anomaly was detected at 51 °C (T_m of probe **1a**). When the proportion of **1a** to DMPC was increased, it was observed that the temperature at which the broad peak occurred became progressively higher and the relative proportion of transition enthalpy of this broad peak increased.

The phase diagram deduced for the DMPC/**1a** system from the calorimetric results is shown in Figure 3. The phase transition of DMPC at about 24 °C remains sharp over most of the concentration, its intensity decreasing progressively with increasing content of the probe **1a**. Thus, the solidus line is indicative of monotectic phase behaviour, that is, of immiscibility in the gel phase. The other transition (liquidus line) occurs at temperatures increasing from 25 to 51 °C as the relative content of **1a** in the mixture increases from 0 to 100%. This implies complete miscibility of the two lipids in the liquid crystalline phase,

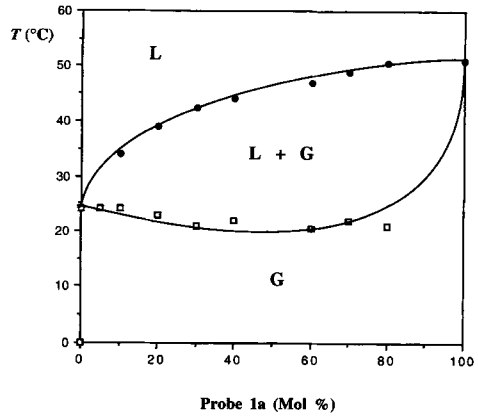

Fig. 3. Phase diagram constructed from calorimetric transition curves for aqueous dispersions of DMPC/**1a**. G: gel state, L: liquid crystalline state.

in which the photochemical experiments in vesicles composed of DMPC/**1a** were performed.

The miscibility properties of binary mixtures of phosphatidylcholines have been studied as a function of the difference in fatty acid chain length (Δ = difference in number of CH_2 groups).[19, 21] A mixture of DMPC and DPPC ($\Delta = 2$) has an almost ideal phase diagram curve. As the difference increases ($\Delta = 4$ or 6), for example, DMPC/DSPC (1,2-distearoyl-*sn*-glycero-3-phosphocholine), DLPC (1,2-dilauroyl-*sn*-glycero-3-phosphocholine)/DSPC, the phase diagram diverges from the ideal curve (monotectic behaviour). The mixture of DMPC and probe **1a** showed monotectic behaviour similar to the case of $\Delta = 6$. This suggests that the phase behaviour of the DMPC/**1a** system is influenced by the "mismatch" between the myristoyl chains of DMPC and the transmembrane core diacid chain of the probe **1a**, though the other regions of the probe **1a** are identical to DMPC.

UV studies of the probe 1a in mixed vesicles with DMPC: The variation of λ_{max} for three vesicle suspensions was measured as a function of temperature (Fig. 4). In agreement with the DSC analysis (Fig. 3), we observed that with increasing amounts of probe **1a**, the phase transition zone shifted towards higher temperatures. The λ_{max} value above the phase transition (284 nm) was found to be slightly lower than that in organic solutions (300 nm in methanol, chloroform, 2-propanol, 1-decanol). A λ_{max} shift of 15 nm is observed below the phase transition as reported for other bilayer systems.[22, 23]

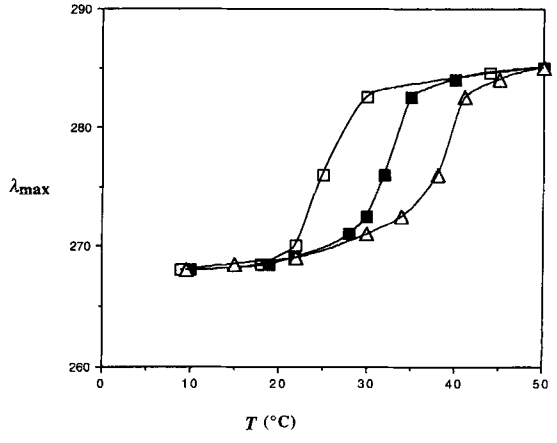

Fig. 4. Variation of the absorption maximum with temperature for different proportions of incorporated **1a**. Vesicles were prepared from DMPC and probe **1a** in the following proportions: □ 4 mol%, ■ 14 mol% and △ 38 mol%.

Study of the orientation of probe ***1b*** *in the DMPC bilayer by solid state ^2H NMR*: In order to define the orientation of the probe in the membrane, the solid state ^2H NMR spectrum was recorded from an oriented multibilayer sample composed of DMPC (90 mol%) and the dideuterated probe **1b** (10 mol%) according to a procedure described previously.[24] The ^2H NMR spectrum of the multibilayer system oriented at 90° to the magnetic field shows two quadrupolar splittings: $\Delta\nu_{QA} = 2.75$ kHz (about 90% intensity) and $\Delta\nu_{QB} = 10.75$ kHz (about 10% intensity) (Fig. 5).

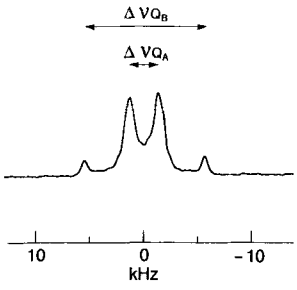

Fig. 5. ^2H NMR spectrum of 90° oriented multibilayers of DMPC/10 mol% probe **1b** at 45 °C.

The quadrupolar splitting $\Delta\nu$ was also measured for different orientations. The curves obtained for the functions $\Delta\nu_{QA}(\theta)/\Delta\nu_{QA}(90°)$ and $\Delta\nu_{QB}(\theta)/\Delta\nu_{QB}(90°)$ both follow a $(3\cos^2\theta - 1)/2$ angular dependence nicely, leading to a minimum when the normal to membrane surface is oriented near the magic angle ($\theta = 54°$; θ: orientation of the normal to the bilayer with respect to the magnetic field). This indicates that there are two different coexisting conformations for the probe **1b**, both with the axis of motional averaging perpendicular to the membrane plane. Because of the internal flexibility and geometry of the benzophenone structure,[25] the assignment of these two splittings to two possible types of conformations for the probe in the bilayer was not easy; however, from the photolabelling results described below, the first splitting (A) was interpreted as corresponding to the transmembrane orientation of the probe **1b**, and the second one (B) to a U form, enabling the benzophenone photoactivable group to "explore" most of the width of the membrane. Additional support for this interpretation was obtained as follows. Knowing that the presence of 33 mol% of cholesterol in the DMPC/probe **1a** vesicles had remarkably increased the regioselectivity of the photolabelling on the myristoyl chains (see later in the photochemical studies), we measured the ^2H NMR spectrum of an oriented multibilayer sample composed of DMPC/cholesterol/probe **1b** (at the molar ratio of 62:33:5) under the same conditions as cited above ($\theta = 90°$, $T = 45$ °C). The quadrupolar splitting corresponding to $\Delta\nu_{QB}$ almost disappeared. This is consistent with the conclusion that almost all probe molecules orient in a transmembrane manner in the presence of 33 mol% of cholesterol.

Other groups have already studied the topographical orientation of two-headed lipids in phosphatidylcholine vesicles by different methods. Phospholipase hydrolysis suggested that the bis-phosphocholine **5** was organized in a U shape,[20] and another study using NMR and electron microscopy suggested that the glycerol dialkyl glycerol tetraether **3** extracted from *Sulfolobus solfataricus* can be accepted into egg phosphocholine vesicles, provided the molecule bends and it is located on the outer layer.[17] Recently, a study using non-membrane-permeating reagents showed that when the dipolar phospholipid **6** was incorporated into vesicles, only about 50% of the molecules were found to be in the desired transmembrane conformation, the other half being incorporated in a U form, 25% in the inner and 25% in the outer leaflets.[15] Therefore, there is an obvious limitation to the use of bipolar molecules. Our success in selecting the transmembrane conformation is probably based on the introduction of a rigid group in the centre of the molecule as suggested in the literature[16] and to the addition of cholesterol to the system.

Influence of the temperature on the line shapes of ^2H NMR spectra: ^2H NMR spectra of the ordered bilayer system composed of probe **1b** (10 mol%) and DMPC (90 mol%) were measured at different temperatures (55, 45, 40, 35, 30, 25 °C; spectra not shown here). Between 55 and 40 °C the spectra were characteristic of those of liquid crystalline phases, and both the intensity of the peaks and $\Delta\nu_Q$ (Δ_{QA} and Δ_{QB}) were unchanged. At 35 °C, $\Delta\nu_Q$ increased and the intensity of the peaks with respect to the intensity of the peak of D_2O which was used as an internal reference diminished (about 90% of that at 55–40 °C). This point is the beginning of the phase transition. At 30 °C, the peak intensity was reduced to about one-half its initial level, that is, the phases were composed of about 50% of the liquid crystalline phase and about 50% of the gel phase. At 25 °C, the peaks were invisible, which implies there was practically no liquid crystalline phase. Using the standard optimum acquisition conditions for the observation of liquid crystalline phases (SW = 250 kHz, DW = 2 μs, recycle time = 52 ms) the liquid immobilized in the gel phase was not observed. These results agree well with those of the phase diagram study described above.

The relaxation times (t_1) were also measured by an inversion-quadrupolar echo sequence with the bilayer normal oriented at 90° to the magnetic field following a procedure described previously;[26] the values of t_1 were 5.1 and 4.3 ms at 45 °C and 6.8 and 5.0 ms at 55 °C for the populations A (transmembrane) and B (U-shape), respectively. The increase of t_1 values upon heating, that is, upon reduction of the correlation time of the movement responsible for t_1 relaxation, indicates that we are on the rapid movement limit ($\omega\tau_c < 1$, that is $\tau_c < 4$ ns) for both conformations.

Influence of the incorporated probe ***1a*** *on the internal mobility of chains of DMPC in the bilayer*: ^2H NMR experiments were also performed with the unlabelled probe **1a** inserted into ^2H labelled DMPC. The order parameters (S_{mol}) (angle 90°, 40 °C) of oriented bilayers of pure 1-myristoyl-2-[D_{27}]myristoyl-*sn*-glycero-3-phosphocholine ([D_{27}]DMPC) and of [D_{27}]DMPC + 10 mol% probe **1a** were compared (Fig. 6). The peak assign-

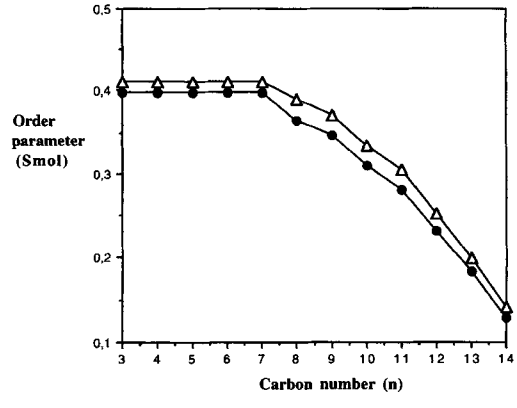

Fig. 6. Order parameter profiles for the [D_{27}]DMPC/probe **1a** (10 mol%) (●) or the pure [D_{27}]DMPC (△) system. The segment order parameter S_{mol} was calculated from the spectra of the 90° oriented multibilayers at 40 °C.

ments of the spectra were obtained on the basis of the peak intensity and on the assumption that S_{mol} decreases monotonically from position 3 to the terminal methyl group as in the case in pure DMPC bilayers.[27]

The order parameter was found to differ by less than 8% at each position of the *sn*-2 myristoyl chain in [D_{27}]DMPC, thus showing that, at 10 mol% concentration, the probe causes very

0947-6539/96/0202-0132 $ 10.00+.25/0 Chem. Eur. J. 1996, 2, No. 2

little perturbation to the internal mobility of DMPC chains in the vesicles. It is important that a probe does not perturb the system to be analyzed, and we have generally used 5 mol% of the probe **1a** for the photolabelling experiments.

Thus, we have demonstrated favourable physicochemical and topographical characteristics of the probes **1a** and **1b** for membrane studies, particularly in the presence of a large quantity of cholesterol, since only one conformation of the probe is then observed.

2. Photochemical studies of the transmembrane photoactivable phospholipid probe on reconstituted vesicles: The efficiency of **1a** as photolabelling probe must now be verified on three points: 1) Does the probe react not only intramolecularly, but also with different surrounding molecular species in the reconstituted vesicle system, that is, do *intermolecular reactions* take place efficiently? 2) Does the probe attack the expected specific sites on the fatty acid chains, that is, near the middle of the bilayer? 3) Does the probe functionalize the expected specific position (C25) on the side-chain of cholesterol? Our photolabelling experiments were performed above the phase transition temperature for 3.5 h in different systems which always contained 5 mol% probe **1a**: POPC/**1a**, DPPC/**1a**, DMPC/**1a** and DMPC/**1a** (5 mol%)/cholesterol (10 mol%, 20 mol% or 33 mol%). The photolabelled products were first analyzed by FAB MS after a transmethylation step, and further chemical degradation steps transformed the products into a series of *n*-oxo fatty acid methyl esters, which were analyzed by GC/MS in order to identify the photolabelled positions on the fatty acid chains. The determination of the functionalized position of the photolabelled cholesterol was performed essentially by NMR.

Intermolecular reaction: Our first aim was to demonstrate the intermolecular reaction between **1a** and another phospholipid component in vesicles such as POPC (1-palmitoyl-2-oleoyl-*sn*-glycero-3-phosphocholine) and DPPC. After UV irradiation of vesicles composed of DPPC (or POPC) and the probe **1a**, followed by transmethylation with MeONa and separation on a Sephadex LH-20 column, the cross-linked samples were analyzed by FAB MS (Fig. 7). The expected molecular species were detected as $[M+H]^+$ or $[M+H-H_2O]^+$ (products dehydrated from the photolysed tertiary alcohols).

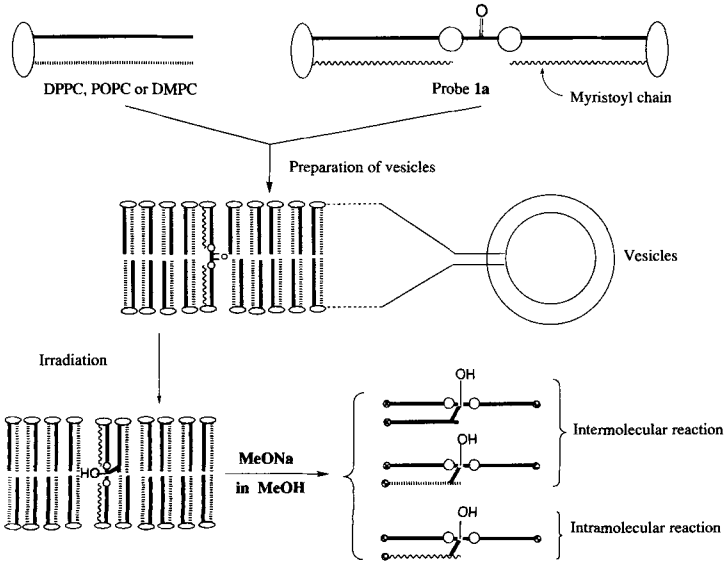

Fig. 7. Photochemistry of the transmembrane probe **1a** in vesicle systems.

Table 2. Selectivity of intermolecular and intramolecular reactions provoked by photolysis, estimated from the intensities of $[M+H]^+$ peak in the FAB mass spectrum.

Vesicle system	Intermolecular reaction m/z for $[M+H]^+$	Intensity	Intramolecular reaction m/z for $[M+H]^+$	Intensity
DPPC/**1a**	863.5 (palmitoyl)	100 (100) [a]	835.5 (myristoyl)	23 (26) [a]
POPC/**1a**	889.5 (oleoyl)	100	835.5 (myristoyl)	11
	863.5 (palmitoyl)	13		

[a] Values obtained by GC.

As expected,[8a] our probe **1a** can attack another lipid component in reconstituted vesicle systems (Table 2). In the DPPC/**1a** system, the intermolecular reaction between **1a** and the palmitoyl chain of DPPC was 4 times more frequently observed than the intramolecular reaction between the core diacid chain and the myristoyl chain on **1a**, by estimation from the peak intensities. This indicates that the intermolecular and intramolecular reactions are almost equally efficient: the expected ratio is 5:1, assuming that the transmembrane chain is surrounded by six fatty acid chains in a hexagonal manner, in which pure lipids can pack as in the L_β phase.[28] This is easily explained in a compact system, where intra- and intermolecular reactions do not differ entropically even in the liquid crystalline state, and where the probe is largely diluted in the phospholipid matrix. This is a crucial result, since it is the intermolecular reaction which will be used for topographical analyses.

In the POPC/**1a** system, the intermolecular reaction between **1a** and the oleoyl chain of POPC is 8–9 times more efficient than the intermolecular reaction between **1a** and the palmitoyl chain on POPC or than the intramolecular reaction (Table 2), while the palmitate:oleate:myristate chain ratio 2.5:2.5:1 was estimated for a compact hexagonal arrangement. In the previous work of Khorana's group, the photolabelling ratio for palmitates at position 1:position 2 of glycerol in DPPC was shown to be 65:35,[6a] and the other cross-linking experiments showed the formation of a covalent bond between the carbene-generating phospholipid probe and DOPC (1,2-dioleoyl-*sn*-glycero-3-phosphocholine) to be twice as efficient as that between the probe and DPPC, while no significant preference was observed between cross-linking to DMPC and DPPC. These results suggest that this preference is based on the preferential reaction of the electrophilic carbene with or near double bonds.[29] Given that radical formation is favoured in allylic positions, the photochemical priority of the fatty acid at the 2 position (oleate) in our work also appears to be caused by the double bond lying in the middle of the oleate chains, and permitted by the disorder prevailing in the absence of cholesterol. However, we have not studied the structure of the products, nor have we checked that the incorporation of cholesterol does reduce the impact of the oleoyl double bond.

For the DMPC/**1a** vesicles, the yield of the cross-linked products (the sum of the intra- and intermolecular couplings) was as high as 60–64% (based on the probe **1a**). Somewhat lower yields (35–40%) were also reported by Lala and Kumar[14b] in their photolabelling experiments on DMPC employing benzophenone-based phospholipids. These yields are better by far than those obtained from hydrophobic photolabelling with carbene or nitrene precursors.[7]

Regioselectivity in systems without cholesterol: Next, the regioselectivity of the photochemistry in fatty acid chains was analyzed according to the procedure described by Breslow et al.[6b, c] (Fig. 8). Chemical degradation (dehydration, oxidative cleavage and diazomethane treatment) of the cross-linked acid methyl esters, which were separated by LH-20 chromatography (vide supra), led to a series of *n*-oxo-fatty acid methyl esters, a small quantity of dimethyl tetradecanedioate and the parent benzophenone-bearing diacid dimethyl ester.

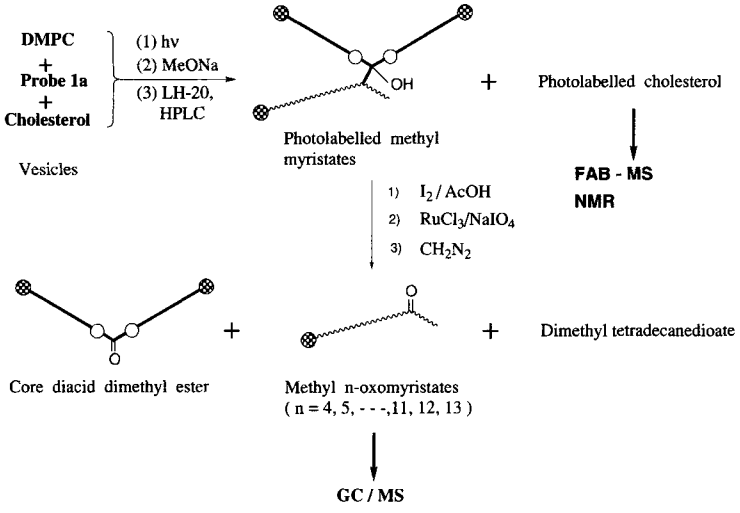

Fig. 8. Scheme of chemical degradations of the photolabelled methyl myristates.

In the DMPC/**1a** system, the major product was methyl 13-oxomyristate (13-oxo MM) (33% yield of functionalization), and the yield of photolabelling decreased gradually as the carbon number on MM (methyl myristate) became lower. The sum of 11-, 12- and 13-oxo MMs exceeded half of the total isomers, which is in agreement with the probe **1a** being predominantly incorporated in a transmembrane conformation. However, 5- and even 4-oxo MMs were also obtained in 4% yield together. This might be due to the presence (10%) of the U-shaped conformations of **1a** in addition to the extensive disorder of the lipid chains. Two different methods of preparation of the DMPC/**1a** system, purified by centrifugation or by filtration through polycarbonate filters, led to no difference in regioselectivity.

In the DPPC/**1a** system, the methyl palmitates (MPs) functionalized on the methylene groups situated near the middle of the bilayer ($\omega-1$ to $\omega-3$-oxo MPs) were less abundant than those observed in the DMPC/**1a** system or in the intramolecular reaction in the DPPC/**1a** system (Table 3). As the probe **1a** was designed to fit the width of the DMPC bilayer, the above result could be explained by the "mismatch" between the length of the hydrophobic part of the probe **1a** and the bilayer width of DPPC.[21c] When we compared the cross-linking on the myristoyl chains in the DPPC/**1a** system with that in the DMPC/**1a** system, no difference in the regioselectivity was observed.

Table 3. Distribution of functionalized carbons on the myristoyl and palmitoyl chains after photolysis (ME = fatty acid methyl ester).

Vesicle system	4- and 5-oxo-MEs (%)	($\omega-3$)-oxo-ME (%)	($\omega-2$)-oxo-ME (%)	($\omega-1$)-oxo-ME (%)
DMPC/**1a** (MMs)	4	11	13	33
DPPC/**1a** (MMs, intra) [a]	5	8	15	33
DPPC/**1a** (MPs, inter) [a]	9	6	10	25

[a] The intramolecular reaction in the DPPC/**1a** system affords functionalized methyl myristates (MMs, intra), while the intermolecular reaction in the same system affords functionalized methyl palmitates (MPs, inter).

In the literature, a disordered distribution was observed for the cross-linked positions using another probe that has two polar head groups and two benzophenone groups in the didodecyl phosphate system.[6b] Recently, in other photolabelling experiments on DMPC vesicles using phospholipidic probes, each of which carries a benzophenone at a different position, a wide range of carbon atoms were functionalized on the myristoyl chains, centred around the expected position.[14b] Although these systems are not the same, the regioselectivity for the photolabelling is much higher in the DMPC/**1a** system than in these earlier cases, justifying the concept of a transmembrane probe. It is, however, still much too low to be of use in structural studies.

The effect of cholesterol: To improve the selectivity of lipid chain cross-linking, we studied the effect of added cholesterol. As summarized in the literature:[1, 2] 1) cholesterol is a ubiquitous membrane reinforcer in eucaryotes, and its content in cellular membranes can reach a phospholipid:cholesterol ratio of 1:1; 2) the ordering effect of cholesterol on membrane lipids in the liquid crystalline state ($T > T_m$) is demonstrated by a reduction in molecular area (monolayers), reduced permeability (vesicles) and reduced mobility of the fatty acid chains (NMR and ESR); 3) it has been suggested that cholesterol is oriented perpendicular to the membrane surface with its hydroxyl group in the aqueous phase and that there are noncovalent attractive interactions between cholesterol and phospholipids leading to 1:1 and/or 1:2 complexes.

The effect of cholesterol was studied in DMPC/**1a** systems that contained this additive in different proportions (Fig. 9). When 10 mol% cholesterol was added, the regioselectivity for the distal end of myristoyl chains increased significantly in comparison with the system without cholesterol; for example, the yield of 13-oxo MM rose from 33% to 42%. When 20 mol% cholesterol was added, the yield of 13-oxo MM increased to more than 60%, and 11–13-oxo MM dominated at 85% of all isomers. Finally, when 33 mol% cholesterol was added, the yield of 13-oxo MM reached 70%, and 11–13-oxo MM domi-

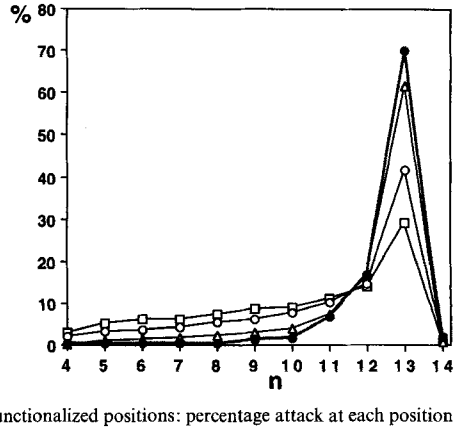

Fig. 9. Distribution of functionalized positions: percentage attack at each position of the myristoyl chain, for example, $n = 1$ (carboxyl); $n = 14$ (C14, position ω). □: In the absence of cholesterol; ○: with 10 mol% cholesterol; △: with 20 mol% cholesterol; ●: with 33 mol% cholesterol.

0947-6539/96/0202-0134 $ 10.00+.25/0 Chem. Eur. J. 1996, 2, No. 2

nated almost completely (95%); the appearance of 4–8-oxo MM was completely repressed. This result was confirmed further by the analysis of the dehydration products of the photolabelled methyl myristate fraction obtained in the photolysis of the DMPC/cholesterol/probe **1a** system (molar ratio: 75:20:5). The mass spectrum of the dehydrated compounds shows, besides the characteristic peaks of *m/z* 775 ($M^+ - CO_2CH_3$) and 595 (the core diacid diester fragment with a transferred 1 H), a series of important peaks (*m/z*: 621, 635, 649, 663, 677, 691, 705, 719, 733, 747, 761) which correspond to allylic fission for compounds functionalized at C14, 13, 12, 11, 10, 9, 8, 7, 6, 5 and 4 on the myristoyl chain, respectively. Among them, by far the strongest peak occurs at an *m/z* value of 635; the second is at 649, and the intensity decreases towards the lower positions. This shows that the ($\omega - 1$) position has been principally attacked, followed by attack at ($\omega - 2$), and other positions have been functionalized less frequently. This result is in good agreement with the analytical results described above for the final chemical degradation compounds using GC/MS.

Only a small amount of dimethyl tetradecanedioate (see Fig. 9) was detected: 0.5% (without cholesterol), 1% (10 mol% of cholesterol), 1% (20 mol%) and 2% (33 mol%), even though the ω-methyl group should lie nearest to the photoactive group. This was expected because attack on the methyl group leads to a primary radical, an unlikely process.

The excellent regioselectivity thus achieved could be explained by the following known facts: 1) the existence of a 1:2 cholesterol/phospholipid association at 33 mol% cholesterol content has been proposed,[28] in which the associated phospholipids can pack in a quasi-hexagonal manner as in their pure gel state, and cholesterol molecules have phospholipids for all their nearest neighbours; 2) ^{2}H NMR studies in the DMPC/30 mol% cholesterol system showed that the cholesterol molecule can be considered as an almost rigid cylinder and that not only the cholesterol nucleus and the methylene units of the fatty acid chain (from C3 to C11) are well ordered, but also the methylene units of the cholesterol side-chain and those at C12 and C13 of the fatty acid are fairly rigid.[30] At 20 mol% cholesterol content, the regioselectivity decreased slightly in comparison with 33 mol%. At 10 mol%, the regioselectivity was greatly decreased. This result suggests that free phospholipids, which are not influenced by cholesterol, exist predominantly in the latter case, while the cholesterol-rich domains contribute to the overall increase in regioselectivity.[28]

Determination of the photolabelled positions on cholesterol: The functionalized cholesterol was partially purified by HPLC from the fraction of cross-linked products (photolabelled methyl myristates (MM*) + photolabelled cholesterol (Ch*)), which had been isolated on a LH-20 column after transmethylation of the photolabelled products from the DMPC/**1a**/33 mol% cholesterol system. A ratio of about 2:1 for MM*:Ch* was estimated by comparing their peak areas in HPLC. The structural analysis of the labelled cholesterols was performed directly using FAB MS and NMR spectroscopy. In the mass spectra, some important peaks (*m/z*: 979.6 $[M + H - H_2O]^+$; 611.3 [*M* – Ch(cholesteryl moiety)]$^+$ (base peak); 595.3 $[M + H - H_2O - Ch]^+$; 319.2 $[CH_3O_2C(CH_2)_{10}C_6H_4CO]^+$) were observed. This shows clearly that cholesterol is cross-linked with the probe **1a** (Fig. 10).

For the determination of the functionalized position(s) on cholesterol, the assignment of the 500 MHz ^{1}H NMR spectrum of the photolabelled cholesterol was achieved by means of HMBC, HMQC, NOESY and ^{1}H–^{1}H COSY experiments and comparison with cholesterol.[31] The methyl proton signals observed at about $\delta = 0.80$ as two doublets for C26 and C27 in cholesterol were shifted about 0.24 ppm downfield and were observed as two singlets (Table 4). A NOE was observed between the methyl protons (C26 and C27) and H_A (C2′) protons on the benzene ring. This indicates that the C25 on the side-chain of cholesterol was functionalized and the benzene ring is located in the vicinity of the above two methyl groups. Furthermore, the HMBC spectrum clearly indicates cross-peaks between the two methyl proton signals (C26, C27) and the carbons (C25, C26/C27, C24, C28). The assignment for the signal at about $\delta = 83$ to C28 was deduced from the presence of a cross-peak between the H_A (C2′) proton signal on the benzene ring and the carbon at C28 (Table 5). From the viewpoint of reactivity (but not of localization) the C20 tertiary position would also be a possible one for photolabelling. In the ^{1}H NMR

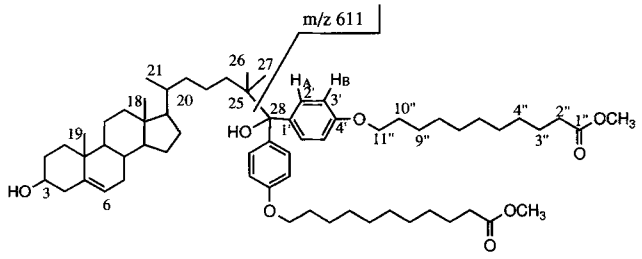

Fig. 10. Structure of the functionalized cholesterol and mass fragmentation for the base peak.

Table 4. NMR data for the functionalized cholesterol (C3, C5, five methyl groups on cholesterol and the attached probe).

Position	^{13}C	^{1}H	Comments
3CH	71.5	3.47(m) [3.45(m)] [a]	HMQC
6CH	121	5.29(d) [5.27(d)]	HMQC
18CH_3	12.0	0.60(s) [0.61(s)]	HMQC
19CH_3	19.5	0.95(s) [0.94(s)]	HMQC
21CH_3	19.0	0.84(d) [0.85(d)]	HMQC
26CH_3	24.0	1.04(s) [0.79(d)]	HMQC, NOESY(with 2′CH_A)
27CH_3	24.0	1.04(s) [0.80(d)]	HMQC, NOESY(with 2′CH_A)
28C	83.0		HMBC (with CH_3 26, 27)
1′C	138		HMBC (with 3′CH_B)
2′CH_A	129	7.32	HMBC, NOESY, COSY
3′CH_B	113	6.72	NOESY (with 11″CH_2), COSY
4′C	157		HMBC (with 3′CH_B)
11″CH_2	67.5	3.86	HMQC, NOESY
10″CH_2	29.5	1.75	HMQC, NOESY, COSY
9′CH_2	26.2	1.42	HMQC, NOESY, COSY
4″CH_2	29.3	1.29	HMBC, NOESY, COSY
3″CH_2	25.2	1.60	HMBC, NOESY, COSY
2″CH_2	33.9	2.24	HMQC, NOESY, COSY
1″CO	175		HMBC (with 2″CH_2 and CH_3O)
CH_3O	50.8	3.61	HMQC

[a] ^{1}H NMR data for cholesterol in square brackets.

Table 5. NMR chemical shifts of methyl or benzene protons and connective carbons of the labelled cholesterol.

CH_3 or $CH_{benzene}$		Connective carbons	
^{1}H	^{13}C	^{13}C-C-H_3	^{13}C-C-C-H_3 or ^{13}C-C=C-H_A
0.60	12.0 (C18)	42.2 (C13)	39.9 (C12), 56.1 (C17), 57.0 (C14)
0.84	19.0 (C21)	36.2 (C20)	56.1 (C17), 37.0 (C22)
0.95	19.5 (C19)	37.5 (C10)	38.3 (C1), 50.2 (C9), 141 (C5)
1.04	24.0 (C26, 27)	42.0 (C25)	24.0 (C26, 27), 38.2 (C24), 83.0 (C28)
7.37	129 (C2′)		83.0 (C28)

spectrum, two methyl proton peaks were observed at $\delta = 1.09$ and 1.10 as singlets with intensities of less than 10% compared with those of the methyl protons at C26 and C27. The former signals could be due to the diastereomeric methyl protons at C21, which might shift downfield about 0.3 ppm as the consequence of the functionalization at C20. However, an unambiguous assignment of these peaks was not possible, and we have observed only one A_2B_2 system in the region of benzene protons, which was assigned as the protons on the benzene rings of the C25 functionalized cholesterol (Table 4).

Thus, we can conclude that the C25 position is principally functionalized by irradiation of the DMPC/**1a**/33 mol% cholesterol vesicles. From simulation and experimental data, the radius of the reactive sphere for a benzophenone is estimated to be 3.1 Å, centred at the ketone oxygen.[32] Taking this assumption into account, our photochemical results indicate that cholesterol is oriented perpendicular to the membrane plane, with the side-chain end located near the middle of the bilayer and the photoactivable group of the probe **1a** in the most centred portion in a highly ordered lipid bilayer structure (Fig. 11).

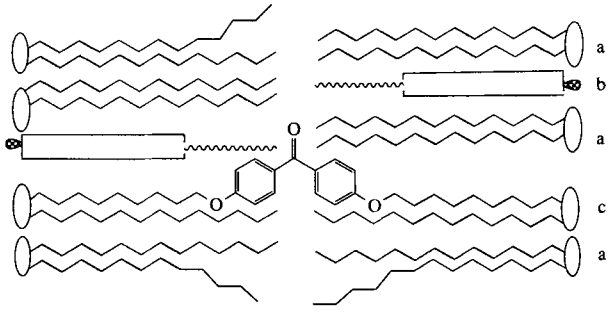

Fig. 11. Schematic presentation of an ordered bilayer system comprised of a phospholipid (a), cholesterol (b) and the transmembrane probe **1a** (c).

Since the work of Breslow's group in the 1970s the *intramolecular* "remote" functionalization of unactivated C–H bonds in sterols has been developed.[10b] However, only one example is known for an *intermolecular* functionalization: Groves and Neumann[3] reported a catalytic C25 regioselective hydroxylation of cholesterol in ca. 2% yield in a biomimetic system of cytochrome P-450, that is, in vesicles using membrane-spanning steroidal metalloporphyrins and oxygen. We have shown here that, in the presence of cholesterol, our novel transmembrane *phospholipidic* probe **1a** gave excellent regioselectivity both with lipid chains and with cholesterol in photolabelling *within* lipid membranes. Studies to define the topography of some membrane-bound proteins are currently under way using this method.

Experimental Procedure

Materials: DMPC and DPPC were obtained from Sigma, POPC from Avanti Polar Lipids; their purity was checked by TLC before use and they were used without further purification. Perdeuterated DMPC ([D_{27}]DMPC) was prepared as described [24b]. Cholesterol was purchased from Aldrich and recrystallized from ethanol before use. The probes **1a** and **1b** were synthesized as reported previously [8c]. 2-Propanol and MeOH were distilled over Mg, AcOH over P_2O_5, and THF over Na. Other chemicals: $RuCl_3 \cdot xH_2O$ (Janssen), $NaIO_4$ (Fluka), 25 wt.% MeONa solution in MeOH (Aldrich), tetradecanedioic acid (EGA), 11-bromoundecanoic acid (Aldrich). Tetradecanedioic acid and 11-bromoundecanoic acid were esterified with diazomethane to give dimethyl tetradecanedioate and methyl 11-bromoundecanoate, respectively. Methyl 13-oxotetradecanoate was prepared by the condensation of ethyl malonate with methyl 11-bromoundecanoate, followed by hydrolysis and decarboxylation. 1,1-Diphenyl-1-tetradecanol was prepared by the condensation of methyl myristate with phenyl magnesium bromide.

Analyses: NMR spectra were recorded on Bruker ARX (500 MHz) or AM (400 MHz) equipment with TMS ($\delta = 0$) and $CHCl_3$ ($\delta = 7.26$) as internal standards for ^1H NMR and $^{13}CDCl_3$ ($\delta = 77.02$) as internal standard for ^{13}C NMR. The chemical shifts are reported in ppm downfield from TMS. Mass spectra were measured on a VG Analytical ZAB-HF double-focusing mass spectrometer in the FAB mode or on a LKB 9000 S apparatus in the GC/MS mode. UV spectra were recorded on a Uvikon 820 Kontron spectrophotometer. Purifications were performed on silica gel (40–63 μm, Merck), Bio-Sil A (200–400 mesh, Bio-Rad) columns by medium pressure chromatography, on a Sephadex LH-20 (Pharmacia) column, or on a silica gel column by HPLC (Waters 486). TLC was carried out on precoated plates of silica gel 60 F 254 (Merck), dipped in a solution of vanillin (1 g) in $EtOH/H_2SO_4$ (95/5, 1 L) and heated on a hot plate to reveal the compounds.

Observation of vesicular structures by optical microscopy: Differential interference contrast (DIC) images of the vesicular structures were taken with an inverted microscope (Axiovert 135, 63x/1.40 Plan-Apochromat Oil DIC objective, Carl Zeiss) connected to a charge coupled device (CCD) camera (C2400-75i, Hamamatsu Photonics), image processor (Argus-20, Hamamatsu Photonics), S-VHS video recorder (SVO-9500MDP, Sony) and video monitor (PVM 1443, Sony). A phospholipid sample (1.0 mg) was dissolved in 350 μL of a 2:1 mixture of chloroform:methanol. An aliquot (1.5 μL) of the solution was dropped onto a microscope slide and allowed to dry for 10 min, after which the lamellar solid remaining on the slide was brought into focus and was hydrated with 1.5 μL of a phosphate buffer (pH 7.3) at 23 °C. Vesicles were observed to grow from the edges of the solid. Alternatively, a suspension of a phospholipid sample prepared by sonication (5 min above T_m in a bath sonicator, Sonorex RK 100H, Bandelin, Berlin) was dropped on a slide and observed. The image of vesicular structures with diameters (d) larger than 0.5 μm can be observed by this technique. For example, we confirmed that the mixture of the probe **1a** and DMPC (92:8 w/w) forms vesicles (photographs not shown here), but vesicular formation ($d > 0.5$ μm) could not be observed from **1a** alone in the two types of preparation.

Preparation of the vesicles:

*For the incorporation or UV study of the probe **1a** in the mixed vesicles with DMPC*: The sonication method was used to prepare small unilamellar vesicles (SUV) [33]. Appropriate aliquots of stock solutions of DMPC (chloroform) and compound **1a** (chloroform/methanol/water, 4:5:1 v/v/v) were mixed and the solvents were evaporated to dryness in vacuo. To this film of mixed lipids (approximately 10 mg) was added 10 mL of buffer (10 mM Tris–HCl, 1 mM $EDTANa_2$, 5 mM NaN_3, "Ultrapure" water from Millipore). This suspension was sonicated under argon for 90 min with a Branson Sonifier B-30 (power setting 5). The vesicle preparation was filtered through polycarbonate filters (Nucleopore, Pleasanton, 0.8, 0.4 and 0.2 μm). The resulting suspension was concentrated to 2 mL in an ultrafiltration cell (Amicon stirred cell). Alternatively, gel filtration of the suspension at 4 °C on a Sepharose 4BCL column (Pharmacia) previously saturated with a fraction of the same solution gave vesicle fractions. Both of these purification procedures eliminate external aggregates. The filtered vesicles (0.7 mg mL^{-1}) were submitted to light-scattering spectrometry at 25 °C on a Coulter N4 MD sub-micron particle analyzer (scattering angle 90°) to measure the vesicles. It was found that 97% of the vesicles had diameters in the range 78–400 nm (160 nm on average). The concentrations of DMPC and compound **1a** in the vesicles were measured by phosphorus determination [34] and by ultraviolet spectroscopy, respectively, after destruction of the vesicles and extraction with chloroform/methanol (1:1 v/v). The two values s (mole% ratio) and r (equivalence% ratio) were calculated according to the relations $s = 100 \times C_{1a}/(C_{DMPC} + C_{1a})$ and $r = 100 \times 2C_{1a}/(C_{DMPC} + 2C_{1a})$, where C_{1a} and C_{DMPC} are the molar concentrations of the probe **1a** and DMPC, respectively. For the measurement of UV spectra the sample was kept at the desired temperature (within ±0.1 °C) for 30 min for equilibration. A series of spectra at several temperatures were taken in heating runs.

For the photolabelling experiments: The lipids and cholesterol were weighed as follows: sample 1: POPC (51.2 mg, 0.067 mmol)/**1a** (5.3 mg, 0.0035 mmol); sample 2: DPPC (95.6 mg, 0.13 mmol)/**1a** (10 mg, 0.068 mmol); sample 3: DMPC (100 mg, 0.15 mmol)/**1a** (11.4 mg, 0.0077 mmol); sample 4: DMPC (104 mg, 0.15 mmol)/**1a** (12 mg, 0.0081 mmol); sample 5: DMPC (90.9 mg, 0.13 mmol)/**1a** (11.8 mg, 0.0080 mmol)/cholesterol (6.1 mg, 0.016 mmol); sample 6: DMPC (69.3 mg, 0.10 mmol)/**1a** (10.1 mg, 0.0068 mmol)/cholesterol (10.5 mg, 0.027 mmol); sample 7: DMPC (54.8 mg, 0.079 mmol)/**1a** (9.4 mg, 0.0064 mmol)/cholesterol (16.2 mg, 0.042 mmol). The lipids were dissolved in $CHCl_3$ (POPC/**1a**, DPPC/**1a**) or the solution of **1a** in $CHCl_3$/MeOH (1:1) was added to the solution of DMPC and cholesterol in $CHCl_3$. After eliminating the solvents by evaporation in vacuo and then hydrating with "Ultrapure" water (50 mL), the mixture was sonicated with a Branson Sonifier B-30 at power level 6–7 in the pulse mode under argon for 40 min; light was excluded with aluminium foil. The crude vesicle preparation was purified by centrifugation (3000 rpm × 5 min) for POPC/**1a** (sample 1), DPPC/**1a** (sample 2), DMPC/**1a** (sample 3), DMPC/**1a**/10 mol% cholesterol (sample 5), or with polycarbonate filters from Nucleopore (0.8 μm × 2, then 0.4 μm × 2) for DMPC/**1a** (sample 4), DMPC/**1a**/20 mol% cholesterol (sample 6) and DMPC/**1a**/33 mol% cholesterol (sample 7) to exclude the metal particles as well as multilamellar vesicles.

0947-6539/96/0202-0136 $ 10.00+.25/0 Chem. Eur. J. 1996, 2, No. 2

Differential scanning calorimetry (DSC): Lipid mixtures were prepared by dissolving the pre-weighed components in a small volume of $CHCl_3$ and removing the solvent first in an argon stream, then in vacuo. 100 µL of "Ultrapure" water was added and the lipids were heated at 60 °C for 1 h. After agitating on a vortex mixer, the suspensions were incubated overnight at 37 °C. Approximately 60 µL of the mixture was sealed in an inox vial and weighed. All calorimetric scans were performed using the Perkin–Elmer DSC-2 B calorimeter, usually at 1.0 K min^{-1} (heating). With pure DMPC, a concentration of 100 mg mL^{-1} was used, with pure probe **1a** a concentration of 116 mg mL^{-1} and with mixtures of lipids, concentrations of 60–300 mg mL^{-1}.

^2H NMR experiments: Preparation of the plates: the plates (cover glasses) were washed in 100% nitric acid for 24 h. They were rinsed 5 times with distilled water, twice with technical acetone and 3 times with pure acetone. They were dried over 12 h at 100 °C. The samples were dissolved in 2-propanol as follows: 1) the dideuterated probe **1b** (21.8 mg, 0.015 mmol, 10 mol%)/DMPC 89.8 mg (0.13 mmol, 90 mol%); 2) probe **1b** (12.0 mg, 0.008 mmol, 5 mol%)/DMPC (104.1 mg, 0.154 mmol, 95 mol%); 3) probe **1b** (12.0 mg, 0.008 mmol, 5 mol%)/DMPC (67.9 mg, 0.100 mmol, 62 mol%)/cholesterol (20.6 mg, 0.050 mmol, 33 mol%); 4) the non-deuterated probe **1a** (1.3 mg, 0.88 nmol, 10 mol%)/$[D_{27}]$DMPC (5.6 mg, 8.0 nmol, 90 mol%). The organic solution was applied dropwise onto clean microscope cover glasses (30–50 plates, 20 × (6–9) × 0.15 mm) and dried under vacuum overnight. The plates were stacked in a 25 × 10 mm NMR tube. The lipids were hydrated by adding about 50 µL of deuterium-depleted water (Janssen), sealing, and letting the stacked plates stand undisturbed. The ^2H NMR experiments were performed with a Bruker MSK 300 spectrometer as described [24]. The observed quadrupolar splitting of a C–D bond with axially symmetric motion is given by:

$$\Delta\nu Q = {}^3/_2(e^2qQ/h)S_{C-D}[(3\cos^2\theta - 1)/2]$$

where e^2qQ/h is the static quadrupolar coupling constant (168 kHz for an aliphatic C–D bond), S_{C-D} the C–D bond order parameter and θ the angle between the symmetry axis for motion and the magnetic field direction ($\theta = 90°$ in the present experiments). A segmental order parameter S_{mol} can be assigned to each labelled position and is expressed as $S_{mol} = -2S_{C-D}$ for the methylene groups and $S_{mol} = -6S_{C-D}$ for the terminal methyl group [27a,35].

Photolysis: The vesicle preparation was placed in a photolysis vessel and the volume was adjusted to 80 mL with "Ultrapure" water. Photolysis with a 125 W medium-pressure mercury lamp (Philips, HPK 125 W) was performed in a quartz well above T_m (at 37 °C for the POPC/**1a**, DMPC/**1a** and DMPC/**1a**/cholesterol systems and at 50 °C for the DPPC/**1a** system) under argon until disappearance of the benzophenone (UV, $\lambda_{max} = 290$ nm). The time required was over 3.5 h for all the systems. The reaction mixture was lyophilized.

Transmethylation and chemical degradation of the photolabelled products: The residue after lyophilization was dried by azeotropic evaporation with 2-propanol (10 mL × 3), then in vacuo and taken up in 0.1 N sodium methoxide (44 mL). After stirring under argon overnight at room temperature, the mixtures were acidified with 10 mL of 1 N HCl [DPPC/**1a**, DMPC/**1a** and DMPC/**1a**/10 mol% cholesterol] neutralized with 4.4 mL of 1 N HCl at 0 °C [POPC/**1a**, DMPC/**1a**, DMPC/**1a**/20 and 33 mol% cholesterol]. After evaporation at RT, the residue was dissolved in CH_2Cl_2 (15 mL) and washed with NaCl-saturated H_2O (10 mL), and the aqueous phase was re-extracted with CH_2Cl_2 (10 mL × 3). The combined organic phase was washed with NaCl-saturated H_2O (10 mL × 3). Evaporation and drying with 2-propanol afforded an oily mixture. Photolabelled products (tertiary alcohols) were sometimes dehydrated by acidification with an excess of 1 N HCl. The oily mixture from the transmethylation step was dissolved in 1 mL of $CHCl_3$/MeOH (1:1) and passed over a Sephadex LH-20 column (1 cm ϕ × 38 cm) with $CHCl_3$/MeOH (1:1) as eluent. Both photolabelled fatty acid methyl esters and photolabelled cholesterols were eluted in higher molecular weight (MW) fractions; nonlabelled products were eluted in lower MW fractions (followed by TLC). Collection and evaporation of the higher MW fractions afforded a mixture of photolabelled products as follows: POPC/**1a** (sample 1): 1.5 mg (from **1a**: 5.1 mg); DPPC/**1a** (sample 2): 2.7 mg (from **1a**: 10.0 mg); DMPC/**1a** (sample 3): 4.1 mg (from **1a**: 11.4 mg), 64% (overall yield based on **1a**); DMPC/**1a** (sample 4): 4.1 mg (from **1a**: 11.8 mg), 60% (overall yield based on **1a**); DMPC/**1a**/10 mol% cholesterol (sample 5): 3.2 mg (from **1a**: 11.8 mg); DMPC/**1a**/20 mol% cholesterol (sample 6): 3.7 mg (from **1a**: 11.8 mg); DMPC/**1a**/33 mol% cholesterol (sample 7): 2.1 mg (from **1a**: 9.4 mg).

In order to separate photolabelled methyl myristates (MM*) and photolabelled cholesterols (Ch*) in the DMPC/**1a**/20 mol% or 30 mol% cholesterol systems, HPLC separation was performed at RT on a silica gel column (Zorbax-z-215, 4.6 mm i.d. × 250 mm, S. F. C. C.) using hexane/ether (1.5:1) as eluent. Other standard operating conditions: peak detection: UV spectrophotometer at 210 nm; elution rate: 1.0 mL min^{-1}. Retention time: MM* 5.0–9.3 min and Ch* 10.5–13.6 min. The ratio of the peak intensities for MM*:Ch* was about 2:1 for both systems. The Ch* peak was collected in two fractions: the ratio of the peak intensities for the first eluted fraction (10.5–11.3 min) and the second (11.3–13.6 min) is about 1:2 for the DMPC/**1a**/20 mol% cholesterol system and 3:7 for the DMPC/**1a**/30 mol% cholesterol system. For the photolabelled cholesterol fractions thus obtained, ^1H NMR spectra showed: sample 6, DMPC/**1a**/20 mol%: first fraction, three A_2B_2 systems in the region of benzene protons, therefore a mixture of different Ch*; second fraction, principally (>80%) C25 photolabelled cholesterol; sample 7, DMPC/**1a**/30 mol% cholesterol: first fraction, principally (about 80%) C25 photolabelled cholesterol; second fraction, principally (>90%) C25 photolabelled cholesterol (see Results and Discussion). FAB MS data (I = 4.6–9.2 V): Sample 1, POPC/**1a**: *m/z*: 889.5 ($[M_1 + H - H_2O]^+$, 77), 863.5 ($[M_2 + H - H_2O]^+$, 6), 835.5 ($[M_3 + H - H_2O]^+$, 3), 611.3 ($[M$ – fatty acid moiety$]^+$, 100), 595.3 ($[M + H - H_2O$ – fatty acid moiety$]^+$, 25). M_1 = photolabelled methyl oleate (MO*), M_2 = photolabelled methyl palmitate (MP*), M_3 = photolabelled methyl myristate (MM*). Sample 2, DPPC/**1a**: *m/z*: 863.6 $[M_1 + H]^+$, 74), 862.6 ($[M_1]^+$, 100), 835.5 ($[M_2 + H]^+$, 15), 834.5 ($[M_2]^+$, 23), 595.4 ($[M + H$ – fatty acid moiety$]^+$, 45). M_1 = dehydrated MP*, M_2 = dehydrated MM*. Sample 5, DMPC/**1a**/10 mol% cholesterol (without HPLC separation): *m/z*: 979.5 ($[M_1 + H - H_2O]^+$, 51), 979.5 ($[M_1 - H_2O]^+$, 80), 835.5 ($[M_2 + H - H_2O]^+$, 30), 834.5 ($[M_2 - H_2O]^+$, 100), 595.3 ($[M_1 + H$ – cholesteryl moiety$]^+$ and/or $[M_2 + H$ – myristoyl moiety$]^+$, 40), M_1 = dehydrated photolabelled cholesterol (Ch*), M_2 = dehydrated MM*. Sample 6, DMPC/**1a**/20 mol% cholesterol (after HPLC separation): photolabelled methyl myristate (MM*): *m/z*: 835.6 ($[M + H - H_2O]^+$, 98), 611.4 ($[M$ – myristoyl moiety$]^+$, 100), 595.4 ($[M + H - H_2O$ – myristoyl moiety$]^+$, 12); photolabelled cholesterol (first fraction): *m/z*: 979.6 ($[M + H - H_2O]^+$, 9), 637.4 (65), 611.4 ($[M$ – cholesteryl moiety$]^+$, 100), 595.3 ($[M + H - H_2O$ – cholesteryl moiety$]^+$, 28) 319.1 ($[CH_3O_2C(CH_2)_{10}C_6H_4CO]^+$, 68); photolabelled cholesterol (second fraction): *m/z*: 979.6 ($[M + H - H_2O]^+$, 20), 700.4 (28), 678.4 (38), 611.3 ($[M$ – cholesteryl moiety$]^+$, 100), 595.3 ($[M + H - H_2O$ – cholesteryl moiety$]^+$, 42) 319.1 ($[CH_3O_2C(CH_2)_{10}C_6H_4CO]^+$, 57). Sample 7, DMPC/**1a**/30 mol% cholesterol (after HPLC separation): photolabelled cholesterol (first fraction): *m/z*: 979.4 ($[M + H - H_2O]^+$, 13), 961.4 ($[M + H - 2H_2O]^+$, 7), 913.1 (11), 611.2 ($[M$ – cholesteryl moiety$]^+$, 100), 595.2 ($[M + H - H_2O$ – cholesteryl moiety$]^+$, 20), 579.2 (7), 333.1 (50), 319.1 ($[CH_3O_2C(CH_2)_{10}C_6H_4CO]^+$, 55); photolabelled cholesterol (second fraction): *m/z*: 979.4 ($[M + H - H_2O]^+$, 13), 961.4 ($[M + H - 2H_2O]^+$, 7), 611.2 ($[M$ – cholesteryl moiety$]^+$, 100), 595.2 ($[M + H - H_2O$ – cholesteryl moiety$]^+$, 22), 579.2 (16), 333.1 (55), 319.1 ($[CH_3O_2C(CH_2)_{10}C_6H_4CO]^+$, 55).

Degradation of the photolabelled fatty acid methyl esters: The mixture of photolabelled methyl myristates (MM*) was dehydrated by stirring with I_2 (cat.) in dry AcOH (10 mL) under reflux for 30 min under Ar. After evaporation, the product was cleaved with $RuCl_3$ (0.6 mg, 0.0029 mmol) and $NaIO_4$ (72 mg, 0.34 mmol) in $CCl_4/CH_3CN/H_2O$ (2:2:3 ml) overnight at RT. The aqueous phase was extracted with CH_2Cl_2 (2 mL × 3). The combined organic phase was washed with $Na_2S_2O_3/H_2O$ (25 mg mL^{-1}, 3 mL × 2), then with 0.1 N HCl (3 mL × 2). After evaporation and drying in vacuo, the residue was dissolved in dry THF (10 mL), CH_2N_2 (1 mL ether solution) was added at 0 °C, and the mixture was stirred for 10 min at 0 °C. After workup with AcOH/THF, evaporation and drying in vacuo gave a mixture of *n*-oxo methyl myristoyl isomers (oxo-MM* isomers), dimethyl tetradecanedioate and the core diacid dimethyl ester (see Fig. 8). The mixtures were submitted to GC and GC/MS analyses. The same chemical and analytical method was applied for the analysis of photolabelled methyl palmitates (MP*). Notes: 1) This procedure was studied and established with 1,1'-diphenyl-1-tetradecanol as a model compound (1 mg) before the real materials were examined. 2) At the dehydration stage, the analysis of dehydrated photolabelled methyl myristates (MM*) was performed by FAB MS for the sample of DMPC/**1a**/20 mol% cholesterol (sample 6): *m/z*: 835.6 ($[M + H]^+$, 100), 803.6 ($[M - OMe]^+$, 5), 635.5 (15), 595.5 ($[M + H$ – myristoyl moiety$]^+$, 9); the following peaks, which are principally derivable from the allylic fission of different dehydrated MM*, were also observed (intensity of the peak at *m/z* = 635.5 as 100): *m/z*: 621.5 (27), 635.5 (100), 649.5 (34), 663.5 (17), 677.5 (13), 691.6 (11), 705.6 (10), 719.6 (10), 733.4 (9), 746.6 (9), 760.6 (10).

Gas chromatography—mass spectrometry analysis (GC/MS): The oxidized fatty acid methyl esters were identified by GC/MS or by GC integration. Cholesterol and *n*-oxo-MM were quantified by GC in comparison with pre-weighed authentic compounds. The pentane or ether solution of the mixture obtained above was injected into a gas chromatograph with a Ross injector. Oxo-MM isomers and/or oxo-MP isomers were chromatographed on a fused silica capillary column (DB 5 30 W, J. & W. Scientific, USA). The column was operated isothermally (150 °C for oxo-MM, 170 °C for oxo-MP), or with a thermal gradient (90–250 °C, 2 ° min^{-1} for oxo-MM, 120–250 °C, 3 ° min^{-1} for oxo-MP, 150–250 °C, 2 ° min^{-1} for methyl tetradecanedioate and 150–300 °C, 8 ° min^{-1} for the quantification of MM and cholesterol. The carrier gas (He) was maintained at 3.6 bar. Other standard operating conditions were: heated inlet temperature, 300 °C; ion source temperature, 300 °C. The resulting effluent vapour from GC was analyzed by EI MS. Mass spectra were obtained at a constant accerating voltage of 3500 V with an electron energy of 70 eV. For this analysis, two authentic comparison samples, methyl 13-oxotetradecanoate and dimethyl tetradecanedioate, were used.

Identification of oxo-fatty acid methyl esters from the mass spectrum: The position of the carbonyl group of oxo-MM isomers is succesfully specified from the mass spectrum by α-cleavage and β-cleavage on either side of the carbonyl

group [36] as follows: α-cleavage: $[M - MeO_2C(CH_2)_mC{=}O]^+$ $(M - \alpha_1)$, $[MeO_2C(CH_2)_mC{=}O]^+$ (α_2) and $[O{=}C(CH_2)_nCH_3]^+$ (α_1); β-cleavage: $[MeO_2C(CH_2)_mC(=O)CH_2+H]^+$ $(M + H - \beta_1)$, $[M - CH_2C(=O)(CH_2)_nCH_3]^+$ $(M - \beta_2)$ and $[CH_2C(=O)(CH_2)_nCH_3+H]^+$ (β_2+H). Other supplemental *m/z* values were carefully checked in comparison with the mass spectra in the literature [36 b] or with the spectra of authentic specimens cited above (Tables 6 and 7).

Table 6. Mass spectral data (*m/z* value) and GC retention time (r.t.) of the methyl oxomyristates (n.d. = not detected).

n-oxo-	r.t.	α_1	M-α_1	α_2	$M + H - \beta_1$	β_2+H	$M - \beta_2$	Other peak [a]
4	27.4	n.d.	115	169	130	n.d.	n.d.	98 [b]
5	27.8	n.d.	129	155	144	n.d.	87	
6	29.8	n.d.	143	141	158	156	101	
7	29.9	n.d.	157	127	172	142	115	
8	30.4	85	171	113	186	128	129	
9	30.7	71	185	99	200	114	143	
10	31.1	57	199	85	214	100	157	
11	31.4	43	213	71	n.d.	86	171	
12	33.6	n.d.	n.d.	57	n.d.	72	185	
13	34.5	n.d.	n.d.	43	n.d.	58	199	

[a] Peaks at *m/z* values of 59, 74, 87, 223 ($[M - 31]^+$) and 254 ($[M]^+$) are specific for the methyl esters of the fatty acid and were detected in all the spectra. [b] This value is specific for the methyl esters of 4-oxo-fatty acids.

Table 7. Mass spectral data (*m/z* value) and GC retention time (r.t., min) of the methyl oxopalmitates (n.d. = not detected).

n-oxo-MM [a]	r.t.	α_1	$M - \alpha_1$	α_2	$M + H - \beta_1$	$\beta_2 + H$	$M - \beta_2$	Other peak [b]
4	28.6	n.d.	115	197	130	n.d.	n.d.	98 [c]
5	28.9	n.d.	129	183	144	n.d.	87	
14	34.3	n.d.	255	57	n.d.	72	213	
15	35.1	n.d.	n.d.	43	n.d.	58	227	

[a] The methyl (6–13)-oxopalmitates were eluted at 30.7–32.2 min and were not well separated under the conditions used. [b] Peaks at *m/z* values of 59, 74, 87, 251 ($[M - 31]^+$) and 282 ($[M]^+$) are specific for the methyl esters of the fatty acid and were detected in all the spectra. [c] This value is specific for the methyl esters of 4-oxo-fatty acids.

Acknowledgements: We are grateful for support granted by the Burkinabé Government (Y. D.), the Herrmann-Schlosser-Stiftung (W. H.), Shin-Etsu Chemical (M. Y.), and CNRS (W. W.). This work was supported in part by the JRDC-ULP "Supermolecules" Joint Research Project. We thank O. Dannenmuller and J. Madden for their valuable help. We are indebted to Mrs. M. Scheer for DSC measurements, to Mr. R. Graf for ^1H and C^{13} NMR experiments, and to Dr. G. Teller and Mr. R. Hueber for MS.

Received: June 21, 1995 [F154]

[1] a) R. A. Demel, B. de Kruyff, *Biochim. Biophys. Acta* **1976**, *457*, 109–132, and references therein; b) P. L. Yeagle, *ibid.* **1985**, *822*, 267–287, and references therein.

[2] M. Rohmer, P. Bouvier, G. Ourisson, *Proc. Natl. Acad. Sci. USA* **1979**, *76*, 847–851.

[3] a) J. M. Groves, R. Neumann, *J. Am. Chem. Soc.* **1987**, *109*, 5045–5047; b) J. M. Groves, R. Neumann, *J. Org. Chem.* **1988**, *53*, 3893–3894; c) J. M. Groves, R. Neumann, *J. Am. Chem. Soc.* **1989**, *111*, 2900–2909.

[4] S. J. Singer, *Annu. Rev. Cell Biol.* **1990**, *6*, 247–296.

[5] a) J. Westerman, K. W. A. Wirtz, T. Berkhout, L. L. M. van Deenen, R. Radhakrishnan, H. G. Khorana, *Eur. J. Biochem.* **1983**, *132*, 441–449; b) L. Ehret-Sabatier, B. Kieffer, M. P. Goeldner, C. G. Hirth, in *Photochemical Probes in Biochemistry* (Ed.: P. E. Nielsen), Kluwer Academic, Dordrecht/Boston/London, **1989**, pp. 107–122.

[6] a) C. M. Gupta, C. E. Costello, H. G. Khorana, *Proc. Natl. Acad. Sci. USA* **1979**, *76*, 3139–3143; b) M. F. Czarniecki, R. Breslow, *J. Am. Chem. Soc.* **1979**, *101*, 3675–3676, c) A. H. Ross, R. Radhakrishnan, R. J. Robson, H. G. Khorana, *J. Biol. Chem.* **1982**, *257*, 4152–4161.

[7] J. Brunner, *Annu. Rev. Biochem.* **1993**, *62*, 483–514, and references therein.

[8] a) Y. L. Diyizou, A. Genevois, Y. Lazrak, G. Wolff, Y. Nakatani, G. Ourisson, *Tetrahedron Lett.* **1987**, *28*, 5743–5746; b) M. Yamamoto, W. A. Warnock, A. Milon, Y. Nakatani, G. Ourisson, *Angew. Chem.* **1993**, *105*, 302; *Angew. Chem. Int. Ed. Engl.* **1993**, *32*, 259–261; c) M. Yamamoto, V. Dollé, W. Warnock, Y. Diyizou, M. Yamada, Y. Nakatani, G. Ourisson, *Bull. Soc. Chim. Fr.* **1994**, *131*, 317–329.

[9] M. De Rosa, A. Gambacorta, B. Nicolaus, B. Chappe, P. Albrecht, *Biochim. Biophys. Acta* **1983**, *753*, 249–256.

[10] a) N. J. Turro, *Molecular Photochemistry*, University Science Books, Mill Valley, **1991**, pp. 255–264 ; b) R. Breslow, *Acc. Chem. Res.* **1980**, *13*, 170–177.

[11] M. B. Ledger, G. Porter, *J. Chem. Soc. Faraday Trans. I* **1972**, *68*, 539–553.

[12] J. N. Pitts, Jr., H. W. Johnson, T. Kuwana, *J. Phys. Chem.* **1962**, *66*, 2456–2461.

[13] a) G. Dorman, G. D. Prestwich, *Biochemistry* **1994**, *33*, 5661–5673; b) K. T. O'Neil, W. F. DeGrado, *Proteins: Structure, Function, and Genetics*, **1989**, *6*, 284–293.

[14] a) C. Montecucco, G. Schiavo, *Biochem. J.* **1986**, *237*, 309–312; b) A. K. Lala, E. R. Kumar, *J. Am. Chem. Soc.* **1993**, *115*, 3982–3988.

[15] J. M. Delfino, S. L. Schreiber, F. M. Richards, *J. Am. Chem. Soc.* **1993**, *115*, 3458–3479.

[16] a) Y. Okahata, T. Kunitake, *J. Am. Chem. Soc.* **1979**, *101*, 5231–5234; b) T. Kunitake, Y. Okahata, M. Shimomura, S. Yasunami, K. Takarabe, *ibid.* **1981**, *103*, 5401–5413.

[17] Z. Mirghani, D. Bertoia, A. Gliozzi, M. D. De Rosa, A. Gambacorta, *Chem. Phys. Lipids* **1990**, *55*, 85–96.

[18] K. Yamauchi, A. Moriya, M. Kinoshita, *Biochim. Biophys. Acta* **1989**, *1003*, 151–160.

[19] S. Mabrey, J. M. Sturtevant, *Proc. Natl. Acad. Sci. USA.* **1976**, *73*, 3862–3866.

[20] E. A. Runquist, G. M. Helmkamp, Jr., *Biochim. Biophys. Acta* **1988**, *940*, 10–20.

[21] a) E. J. Shimshick, H. McConnell, *Biochemistry* **1973**, *12*, 2351–2360; b) P. W. M. van Dijck, A. J. Kaper, H. A. J. Oonk, J. De Gier, *Biochim. Biophys. Acta* **1977**, *470*, 58–69; c) D. A. Wilkinson, J. F. Nagle, *Biochemistry* **1979**, *18*, 4244–4249; d) R. N. McElhaney, *Chem. Phys. Lipids* **1982**, *30*, 229–259; e) I. P. Sugar, G. Monticelli, *Biophys. J.* **1985**, *48*, 283–288; f) S. Massari, R. Colonna, *Biochim. Biophys. Acta* **1986**, *863*, 264–276; g) J. H. Ipsen, O. G. Mouritsen, *Biochim. Biophys. Acta* **1988**, *944*, 121–134.

[22] M. Shimomura, T. Kunitake, *Chem. Lett.* **1981**, 1001–1004.

[23] A. Milon, G. Wolff, G. Ourisson, Y. Nakatani, *Helv. Chim. Acta* **1986**, *69*, 12–24.

[24] a) I. Schuler, A. Milon, Y. Nakatani, G. Ourisson, A. M. Albrecht, P. Benveniste, M. A. Hartmann, *Proc. Natl. Acad. Sci. USA* **1991**, *88*, 6926–6930, b) M. A. Krajewski-Bertrand, A. Milon, Y. Nakatani, G. Ourisson, *Biochim. Biophys. Acta.***1992**, *1105*, 213–220.

[25] a) Z. Rappoport, S. E. Biali, M. Kaftory, *J. Am. Chem. Soc.* **1990**, *112*, 7742–7748; b) K. M. Gough, T. A. Wildman, *ibid.* **1990**, *112*, 9141–9144.

[26] M. A. Krajewski-Bertrand, Y. Nakatani, G. Ourisson, E. J. Dufourc, A. Milon, *J. Chim. Phys.* **1992**, *89*, 237–242.

[27] a) J. Seelig, *Q. Rev. Biophys.* **1977** *10*, 353–418; b) E. Oldfield, M. Meadows, D. Rice, R. Jacobs, *Biochemistry* **1978**, *17*, 2727–2740.

[28] a) H. Lecuyer, D. G. Dervichian, *J. Mol. Biol.* **1969**, *45*, 39–57; b) D. M. Engelman, J. E. Rotham, *J. Biol. Chem.* **1972**, *247*, 3694–3697; c) H. J. Hinz, J. M. Sturtevant, *ibid.* **1972**, *247*, 3697–3700; d) P. B. Hitchcock, R. Mason, K. M. Thomas, *J. Chem. Soc. Chem. Commun.* **1974**, 539–540; e) M. Elder, P. Hitchcock, F. R. S. Mason, R. G. G. Shipley, *Proc. R. Soc. London Ser. A.* **1977**, *354*, 157–170; f) F. T. Presti, R. J. Pace, S. I. Chan, *Biochemistry* **1982**, *21*, 3831–3835.

[29] W. Curatolo, R. Radhakrishnan, C. M. Gupta, H. G. Khorana, *Biochemistry* **1981**, *20*, 1374–1378.

[30] E. J. Dufourc, E. J. Parish, S. Chitrakorn, I. C. P. Smith, *Biochemistry* **1984**, *23*, 6062–6071.

[31] S Seo, H. Saito, A. Uomori, Y. Yoshimura, K. Toda, Y. Nishibe, M. Hirata, Y. Takeuchi, K. Takeda, H. Noguchi, Y. Ebizuka, U. Sankawa, H. Seto, *J. Chem. Soc. Perkin Trans. 1* **1991**, 2065–2072.

[32] M. A. Winnick, *Acc. Chem. Res.* **1977**, *10*, 173–179.

[33] C. H. Huang, *Biochemistry* **1969**, *8*, 344–351.

[34] P. S. Chen, Jr., T. V. Toribara, H. Warner, *Anal. Chem.* **1956**, *28*, 1756–1758.

[35] a) G. W. Stockton, I. C. P. Smith, *Chem. Phys. Lipids* **1976**, *17*, 251–263; b) G. W. Stockton, C. F. Polnaszek, A. P. Tulloch, F. Hansan, I. C. P. Smith, *Biochemistry* **1976**, *15*, 954–966.

[36] a) J. R. Dias, C. Djerassi, *Org. Mass Spectrom.* **1972**, *6*, 385–406; b) J. L. Weihrauch, C. R. Brewington, D. P. Schwartz, *Lipids* **1974**, *9*, 883–890.

0947-6539/96/0202-0138 $ 10.00+.25/0